Cornell University
College of Engineering

School of Civil and
Environmental Engineering
Peter Diamessis
Associate Professor
Environmental Fluid Mechanics and
Hydrology
105 Hollister Hall
Ithaca, NY 14853
Tel: 1-607-255-1719
Fax: 1-607-255-9004
e-mail: pjd38@cornell.edu
website: www.cee.cornell.edu/pjd38

Ithaca, NY, April 17, 2017

Defense Technical Information Center
8725 John J. Kingman Road Ste 0944
Fort Belvoir, VA 22060-6218

To Whom It May Concern:

Please find attached my final report for the O.N.R.-Turbulence and Stratified Wakes-funded project titled "Reynolds Number Scaling and Parameterization of Stratified Turbulent Wakes" (Award Number: N00014-13-1-0665).

Please let me know if you would like any additional information from me.

Sincerely,

Peter Diamessis

REPORT DOCUMENTATION PAGE

Form Approved
OMB No. 0704-0188

Public reporting burden for this collection of information is estimated to average 1 hour per response, including the time for reviewing instructions, searching data sources, gathering and maintaining the data needed, and completing and reviewing the collection of information. Send comments regarding this burden estimate or any other aspect of this collection of information, including suggestions for reducing this burden to Washington Headquarters Service, Directorate for Information Operations and Reports, 1215 Jefferson Davis Highway, Suite 1204, Arlington, VA 22202-4302, and to the Office of Management and Budget, Paperwork Reduction Project (0704-0188) Washington, DC 20503.
PLEASE DO NOT RETURN YOUR FORM TO THE ABOVE ADDRESS.

1. REPORT DATE *(DD-MM-YYYY)*	2. REPORT TYPE	3. DATES COVERED *(From - To)*
04/17/2017	Final Technical Report	07/01/2013 to 12/31/2016

4. TITLE AND SUBTITLE
Reynolds Number Scaling and Parameterization of Stratified Turbulent Wakes)

5a. CONTRACT NUMBER

5b. GRANT NUMBER
N00014-13-1-0665

5c. PROGRAM ELEMENT NUMBER

6. AUTHOR(S)
Diamessis, Peter J.

5d. PROJECT NUMBER

5e. TASK NUMBER

5f. WORK UNIT NUMBER

7. PERFORMING ORGANIZATION NAME(S) AND ADDRESS(ES)
School of Civil and Environmental Engineering
220 Hollister Hall
Cornell University
Ithaca, NY 14853

8. PERFORMING ORGANIZATION REPORT NUMBER

9. SPONSORING/MONITORING AGENCY NAME(S) AND ADDRESS(ES)
Office of Naval Research
875 North Randolph Street
Arlington, VA 22203-1995

10. SPONSOR/MONITOR'S ACRONYM(S)
O.N.R.

11. SPONSORING/MONITORING AGENCY REPORT NUMBER

12. DISTRIBUTION AVAILABILITY STATEMENT
Approved for public release; distribution is unlimited.

13. SUPPLEMENTARY NOTES

14. ABSTRACT
The work funded by this grant has examined both the turbulence and the internal wave field emitted by a stratified turbulent wake of a towed sphere over a range of body-based Reynolds and Froude numbers using implicit Large Eddy Simulation (LES). Work has been completed on the Lagrangian drift, and hence particulate dispersion, induced by a internal wave beam reflecting off a rigid lid surface in an idealized linear stratification.The far-field and surface signature of the internal wave field emitted by stratified turbulent wakes has also been examined. Simple predictor models linking surface-observed wavelengths to body-generating depth and passage time have been constructed. High Reynolds/Froude number wakes are found to induce remotely detectable signatures via slick formation or surface particle drift. Finally, enabled by a Frontier grant, an additional suite of LES at an even higher Reynolds number has been conducted. Preliminary analysis has shown the first-ever Reynolds-number-based prediction-focused scaling for wake-turbulence and the persistence time of energetic wake signatures.

15. SUBJECT TERMS
Stratified turbulent wakes, high Reynolds numbers, internal waves, nonlinear effects, mean flows, Lagrangian dispersion.

16. SECURITY CLASSIFICATION OF:			17. LIMITATION OF ABSTRACT	18. NUMBER OF PAGES	19a. NAME OF RESPONSIBLE PERSON
a. REPORT	b. ABSTRACT	c. THIS PAGE	SAR	18	Peter J. Diamessis
U	U	U			19b. TELEPONE NUMBER *(Include area code)* 607-255-1719

FINAL REPORT, April 14, 2017

Contract Information

Contract Number	N00014-13-1-0665
Title of Research	Reynolds Number Scaling and Parameterization of Stratified Turbulent Wakes
Principal Investigator	P. J. Diamessis
Organization	School of Civil and Environmental Engineering, Cornell University
Contracting Officer	Dr. Ronald Joslin (transitioned to Dr. Thomas Fu)

Technical Section

Technical Objectives

The research supported by ONR grant number N00014-13-1-0665 was conducted in two phases, as the initial stages of this effort involved closing significant research on the subsurface signature of wake-radiated internal waves. The primary objectives of each phase are listed below.

STAGE-1, "Subsurface Signature of the Internal Wave Field Radiated by Submerged High Reynolds Number Stratified Wakes":

- Characterize the low-wind-condition subsurface signature of a single high-frequency internal wave beam(s) in a uniform or vertically variable stratification, the latter typical of littoral ocean conditions.
- Correlate qualitatively and quantitatively, over a range of Reynolds and Froude numbers, the patterns of subsurface motion observed above a stratified turbulent wake with the flow patterns inside the wake core to infer the state ("age") of wake turbulence.

STAGE-2, "Reynolds number scaling of Stratified Turbulent Wakes":

- Identify the Reynolds number scaling for Non-Equilibrium (NEQ) regime duration, diagnostics of secondary turbulence, vertical momentum flux and radiated internal wave properties in a stratified turbulent wake.
- Develop Reynolds/Froude number parameterizations of associated vertical transport coefficients for use in RANS and self-similarity-based models ; assess the accuracy of the latter by comparing with LES results.

Note that, prior to its originally planned termination for 12/31/2016, on account of changes in the ONR logistical systems, this project was replaced in late Spring 2015 by award N00014-15-1-2513, titled "High Reynolds Number Stratified Turbulent Wakes: Internal Wave Energetics, Self-Similarity and Subgrid-Scale Modeling". The objectives of this new award essentially overlap with and extend those listed in STAGE-2 above.

Results

The results obtained in pursuit of the above objectives may be grouped in the following categories, on each of which we further elaborate below:

(i) Lagrangian flows in the reflection of an internal wave beam off a free-slip surface.
(ii) Surface/subsurface signature of the wake-radiated internal wave field.
(iii) High Reynolds number stratified wakes.
(iv) Collaborative DNS/LES of high Reynolds number stratified wakes (Frontier-award support).

(i) Lagrangian flows in the reflection of an internal wave beam off a free-slip surface.

A significant part of the previous grant involved the quantification of mean flows in the reflection region of an internal wave beam (IWB) incident on a free-slip surface, for a linear stratification either extending to the top or with a mixed layer overlaying it (see schematic in Figure 1). Results on mean flow scaling and parameterization and comparison with theoretical findings of a group in MIT were published previously by Zhou and Diamessis (*Phys. Fluids* 2013) through previous ONR support. However, a perplexing question was repeatedly posed to the PI and PhD student at conferences: Are these mean flows Eulerian or Lagrangian in nature ? Any wave-driven flow has associated with it a Stokes drift, i.e. the velocity linked to the residual displacement of a particle after it has completed one full cycle of its orbit over one wave period. The Stokes drift is very likely to counterbalance the Eulerian mean flow, and the true Lagrangian mean may be dramatically different than what our previous study proposed.

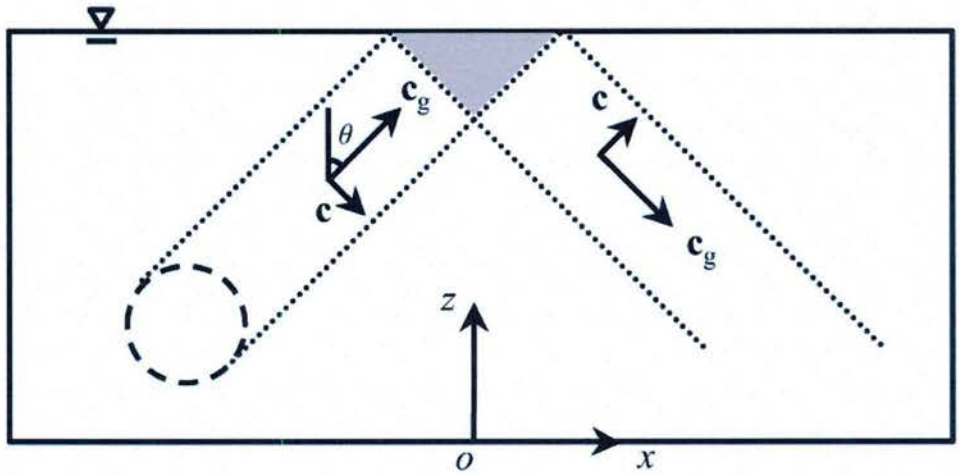

Figure 1. Schematic of the reflection of an internal wave beam (IWB) off a free-slip surface. The beam is incident at an angle θ to the vertical. The shaded region is the location where nonlinear dynamics and, therefore, Lagrangian mean drift are most potent.

An extensive existing database of 19 2-D simulations of free-slip reflecting IWBs in linear stratifications was to quantify the Lagrangian flows in the reflection region. The parameters typically varied were the

IWB amplitude, inclination θ to the vertical and beam compactness (wavelengths contained in the beam envelope).

Straightforward theoretical analysis shows that an $O(A)$ IWB beam (here A is a measure of the beam amplitude, typically given by its steepness, i.e., max. isopycnal displacement normalized by horizontal wavelength) generates an $O(A^2)$ mean flow and an $O(A^2)$ first harmonic in the reflection zone. Moreover, one can show motions of $O(A^n)$ can produce a $O(A^{n+1})$ Stokes drift. In particular, analytical estimation of the Stokes drift in the *inviscid* theoretical surrogate of our modeled IWB indicates that it exactly *cancels out* the Eulerian mean flow for all beams considered. In other words, at least on a theoretical level, no mean transport of surface particulates should be expected in the (sub)surface zone.

Nevertheless, the theoretical beam neglects both viscous effects but also higher-order effects. Hence, we performed Lagrangian particle tracking on all of the above 19 datasets. The particle tracking algorithm is based on spectral interpolation in space in the horizontal (Fourier) and vertical (multidomain-based Legendre/Lagrange). Additionally, it employs an $O(\Delta t^4)$ Adams-Bashforth-Moulton scheme in time. The high spatiotemporal accuracy is paramount to produce reliable results over the long-time integrations associated with the monitoring of each particle. Parallel implementation of the algorithm has been enabled through use of par-for loops in Matlab.

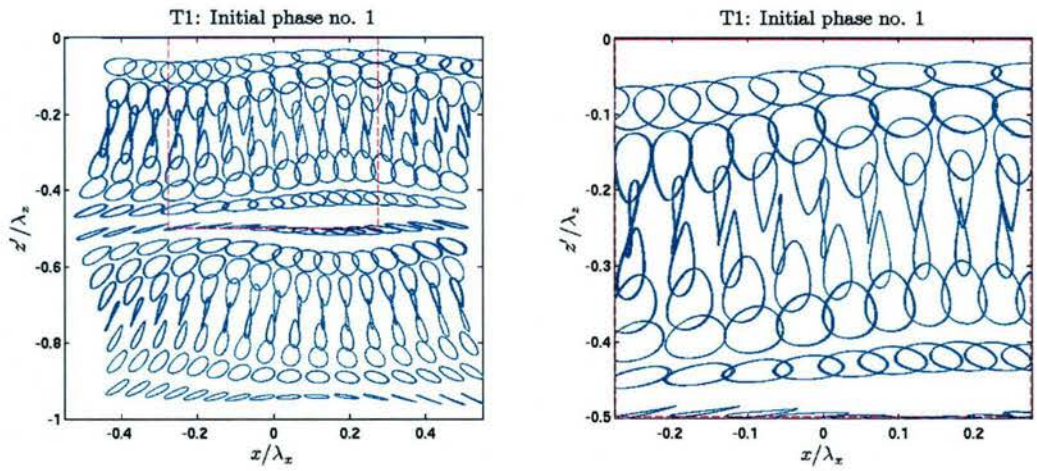

Figure 2. Typical *type-A* particle orbits from from T01 (A = 3.23% and $\theta = 45^0$). Trajectories of a two-dimensional array of 16×16 = 256 particles are plotted over five wave periods. Left panel shows the full field of view spanned by the original array of particles ; right panel shows a zoomed-in view within the dashed-line box drawn in the left panel. The drifts in the mean orbital position are so small that orbits from five periods effectively overlap into one closed trajectory. overlap onto one, for each initial position.

Within the reflection zone, over a region of dimension $\lambda_x \times \lambda_z$ (λ_x and λ_z are the wavelengths in the horizontal and vertical direction, respectively) square array of 16×16 particles is inserted over 18 equally spaced intervals within one wave period. This total of of 4,068 particles is tracked over the course of five IWB periods generating the desired Lagrangian statistics.

We have classified our simulations into three broader categories, based on the observed particle orbits within the reflection region (Figures 2 to 4). Type-A trajectories, typical of lower-amplitude IWBs oriented closer to the vertical are fairly regular and closed, i.e., no net drift of the particles is observed. As the beam orientation is moved away further from the vertical, at an inclination angle θ=63°, a weak drift is observed in the particle position of the order of $0.01\lambda_x$. Such particle orbits are regarded as Type-B. At the same value of θ and with only a twofold increase in IWB amplitude, the drift becomes stronger and particle orbits, regarded as Type-C, are subject to significant distortions.

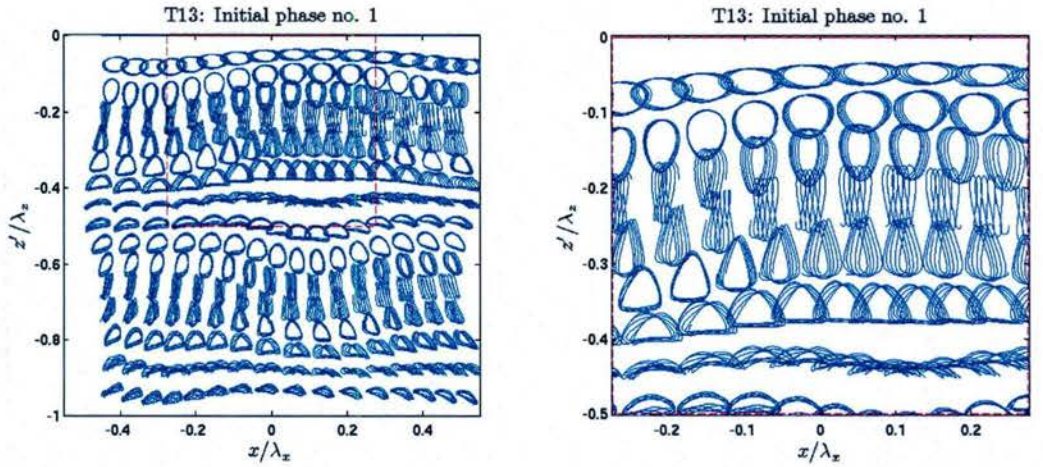

Figure 3: Typical *type-B* particle orbits from from T01 (A = 1.27% and θ = 63°). A net drift can now be observed for each initial position, while the orbital shape remains repeatable from one wave cycle to the next.

Depth-averaged values of the mean and rms IWB-mean Lagrangian drifts (not shown here) show that in the mean, the net drift is not that powerful because of variations in its sign in the vertical direction. However, the rms value of the Lagrangian drift is significant, reaching as high as 10% of the IWB phase speed. Figure 5 (left panel) shows the maximum rms value of the Lagrangian (sum of Eulerian and Stokes) drift velocity U_L as a function of $A\tan\theta$, a parameter which successfully scaled the Eulerian mean flows investigated in our previous studies. Unlike the theoretical estimate, U_L is not zero but scales a A^2, although it is much weaker than its Eulerian contribution (Figure 5) with which it follows the same power law behavior. Moreover, when normalized by the horizontal phase speed, c_x, it can get reach values as high as 10%.

The occurrence of strong rms values of the Lagrangian drift vs. significantly lower mean values of it, suggests that although there might not be a collective horizontal drift of particles across the water column, significant particle dispersion will indeed take place. This dispersion may be quantified in the form of a horizontal dispersion coefficient, K_x, defined by $\sigma^2=2K_x\Delta t$ where σ is the variance of particle displacements over a characteristic time Δt, taken to be one or multiple wave period(s). Straightforward arguments show that K_x scales as A^4 as is indeed confirmed by our data for Δt equal to 5 wave periods (Figure 5 right panel).

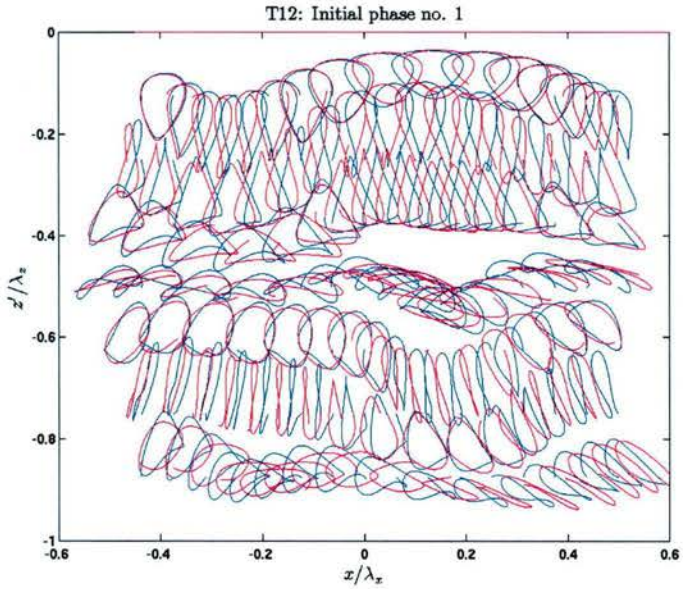

Figure 4: Typical *type-C* particle orbits from from T01 ($A = 2.65\%$ and $\theta = 63^{\circ}$). Particle orbits are shown for two wave cycles only: Trajectories during the first cycle are drawn in blue, and the immediately following cycle in red. Particles are downsampled in the vertical for clarity. The orbital shape of some particles varies from the previous wave cycle to the next, and a great amount of net drift in the mean orbital position can be observed.

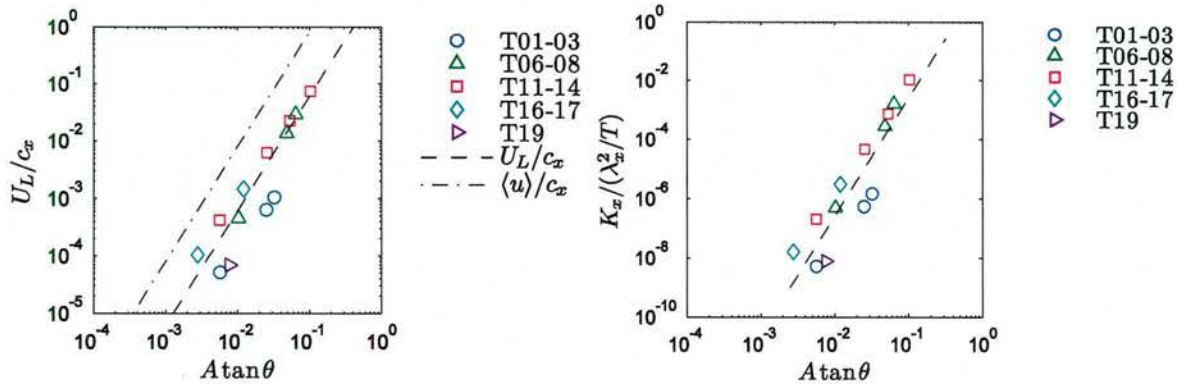

Figure 5: Left panel: Quadratic scaling $U_L/cx \sim (A\tan\theta)^2$ of Lagrangian mean drift velocity scale U_L. Dash line is the quadratic fit for all data points of U_L/cx against $A\tan\theta$; dash-dot line is the theoretical scaling of Eulerian mean flow $\langle u\rangle/cx = 8\pi^2(A\tan\theta)^2$ computed in previous ONR-funded work. Right panel: Quartic scaling $K_x/(\lambda_x/T)^2 \sim (A\tan\theta)^4$ of dispersion coefficient Kx within a reflecting IWB. Dash line represents power law $(A\tan\theta)^4$.

The question that naturally arises is how one might relate these results to the surface reflection of wake-radiated internal waves, under at least the common assumption that an IWB is a reliable first-order surrogate of such waves ? In past work, we have found that the internal waves generated by stratified sphere wakes have horizontal wavelengths λ_x in the range $[D,3D]$ for $4 \leq Fr \leq 64$. The wave orientation angle increases up to θ=55° for higher Re wakes, with these waves potentially assuming an even more horizontal inclination at Re values not accessible to parallel LES nowadays. For these same waves we

have also found that $c_x \approx 0.01U$, where U is the sphere tow speed. Extrapolating the above to operational conditions, where $D \approx 10$m and $U \approx 10$m/s, this suggests a Lagrangian drift velocity of $U_L \approx 0.001U = 1$ cm/s . Given that internal wave periods are typically a factor of two longer than the ambient buoyancy period N^{-1}, with typically $0.01<N<0.001$ Hz one might expect drifts of 5 to 50m over five buoyancy periods. Our dispersion coefficient estimates suggest that these drifts will be accompanied by average particle displacements of $\sigma = (10K_xT)^{1/2} = 10^{-1}\lambda_x T = \approx O(10\text{m})$.

Our findings on Lagrangian drifts and dispersion caused by a reflecting internal wave beam may be found in the article by *Zhou and Diamessis* (*Phys. Fluids* 2015).

(ii) Surface/subsurface signature of the wake-radiated internal wave field.

An extensive analysis of six LES datasets in very deep and wide domains was performed to explore the signature of wake-radiated internal waves on an rigid lid surface within an idealized linear stratification. The datasets span parameter values of internal Froude number, Fr=4, 16 and 64, and two values of $Re=5\times10^3$ and 10^5. The problem geometry is shown in Figure 6, which shows a schematic of an Oyz transect. The stratification used is always linear, as more complex stratifications (e.g. pycnocline) and background currents are issues that will considered in future studies.

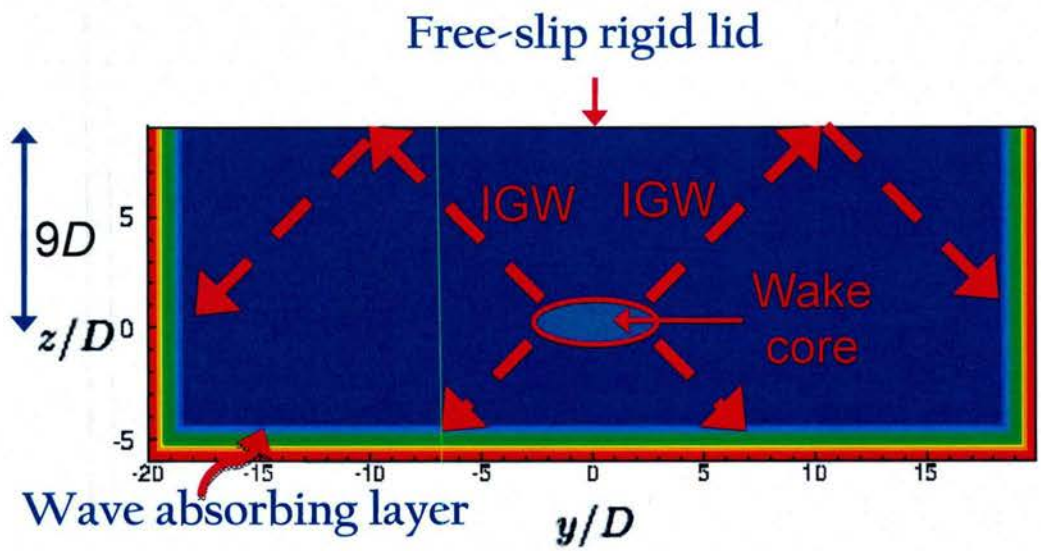

Figure 6: Schematic of a span-depth cross-section of the computational domain used in the LES of the (sub)surface signature of wake-radiated IWs. The wake core is located at the same depth of 9*D* for all runs, whereas the domain is sufficiently wide to allow for the surface reflection of the wake-emitted waves which eventually dissipated in the absorbing layers.

A fundamental pillar in the analysis of the surface-reflecting wake-emitted internal wave field are 1-D and 2-D wavelets. 1-D Morlet wavelets are used to compute the dominant internal wave frequency as a function of spanwise offset and time. 2-D Morlet (non-directionally biased) wavelets are used to identify the horizontal internal wave lengths at the surface. Details of the computation procedure are reported in the thesis of the recently graduated PhD student supported by this grant.

2-D wavelet analysis of the surface-reflecting internal wave field, exploiting the homogeneity of the streamwise direction, generates a number of data points in a 3-D volume in the space (y/D, λ_H/D, Nt) where y/D and λ_H/D are the non-dimensional spanwise offset and horizontal wavelength, respectively. This volume of data may be collapsed along the y direction, as λ_H is not found to exhibit a strong transverse dependence (unlike the actual frequency which is typical of a highly dispersive wave field). A joint p.d.f. in the (λ_H/D, Nt) may then be constructed, as shown in Figure 7. The peak values of joint p.d.f.'s correspond to the energetic internal waves with the most frequently occurring wavelength impacting the free surface and straining it accordingly. At a given Re, the energetic packets arrive at the surface at a later time as Fr is reduced. For a given Fr, the arrival time is shifted in time towards a later Nt. Finally, the most frequently occurring wavelengths appear to lie along a universal line with the location of the centers of the joint p.d.f. contours varying as a function of (Re,Fr).

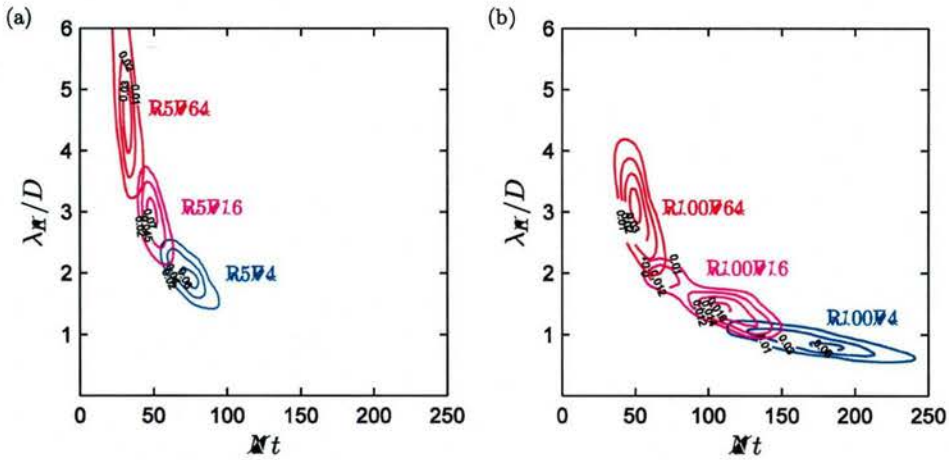

Figure 7: Joint probability density contours of most energetic wave packets in the (λ_H/D,Nt) sample space at *(a)* $Re = 5 \times 10^3$ and *(b)* $Re = 10^5$ respectively for $Fr \in \{4, 16, 64\}$.

At a given Nt, one can average along λ_H/D, for values of probability density exceeding a certain threshold. Figure 8 shows the evolution of the resulting conditionally-averaged mean horizontal wavelength $\overline{\lambda_H} / D$ across all six cases considered. The evolution of $\overline{\lambda_H}$ follows a universal trend, for all simulations performed, described by a $(Nt)^{-1}$ power law. Such a power law is consistent with the findings of previous experimental studies and motivates one to revert to linear theory.

The definition of the vertical group velocity, according to linear theory, ultimately leads to a relationship between λ_H/D and the origin, z_0, of the wake-radiated internal waves and their angle of propagation, θ:

$$\frac{\lambda_H}{D} = \frac{z - z_0}{D} \frac{2\pi}{\sin\theta \cos^2\theta} \frac{1}{N(t - t_0)}$$

Here z=0 corresponds to the wake centerline. If one assumes that $t >> t_0$, i.e., significant time has elapsed since the waves were emitted and, when impacting the free surface, they are in the "far-field" w/r to the wake core, λ_H/D may be approximated as:

$$\approx \frac{z - z_0}{D} \frac{2\pi}{\sin\theta \cos^2\theta} \frac{1}{Nt}.$$

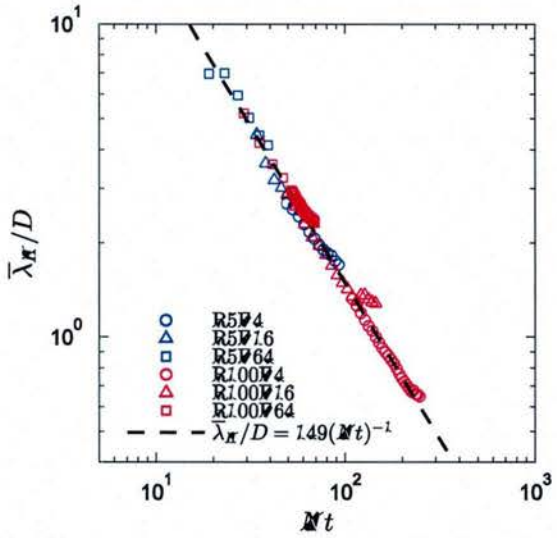

Figure 8: Time series of conditionally averaged wavelengths $\overline{\lambda_H}/D$ observed at the sea surface. Best fit to the linear propagation model is shown as dash line.

Notice how a $(Nt)^{-1}$ power law is recovered from purely linear theory. This finding suggests that the key process driving the dynamics of the internal waves upon arrival at the free surface is linear dispersion. In other words, at least for the *Re* and *Fr* considered here, the far-field behavior of the wake-emitted internal waves is *linear* ; any non-linearities are restricted to the near-field region, immediately around the wake edge. Any non-linear effects at the surface originate from the interaction of an incident packet with its reflecting counterpart and not any interactions among upward propagating wave packets.

Can any prediction be made on the depth of the wave-generating wake based on surface information, namely measured values of λ_H/D ? To this end, a schematic is given in Figure 9. Consider the surface depth of z=9D that holds for all the simulations considered here. The surface needs to be placed sufficiently far from the wave-generating turbulence for the above equation to hold, i.e., the waves need to propagate over a sufficiently long distance to actually disperse. Now, considering a typical value of θ=45° and using a least-squares fit power law for the data in Figure 8, one finds that $z_0/D = 0.62 \pm 0.11$. The "virtual origin" of the waves z_0 should not be confused with the actual wake edge and is, instead, a calibration parameter of our linear model, much like a virtual origin may be identified for a wake or jet by relying on the corresponding self-similarity solution.

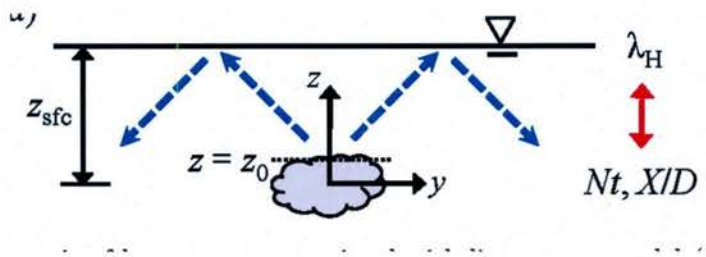

Figure 9: Schematic of key concepts associated with our linear wave model for wake-radiated internal wave propagation as evaluated at the sea surface ($z = z_{sfc}$). Internal waves (dash arrows) of various wavelengths λ_H are observed at the surface as if they had been emitted from the virtual origin z_0 at $t_0 \ll t$. The linear model relates the surface observed λ_H to the submerged turbulence characterized by the dimensionless time Nt since the passage of the wake-generating body.

Nevertheless, returning to the original question above, inferring Nt solely from λ_H/D is not possible as the depth of the wake centerline from the free surface is also needed. For any combination of (Re,Fr), the linear theory-based evolution curve of λ_H/D could lie along any of multiple curves whose offset depends on the depth of the wake core (Figure 10). In more practical terms, given a surface observation of wavelength, the passage time and depth of the wake-generated body cannot be inferred simultaneously ; at least one of these quantities must be known a priori. One must know the depth to compute how much time (in Nt units) has elapsed since the passage of the body. Alternatively, the passage time must be needed to estimate the depth of the wave source. In both cases, priori knowledge of the deeper water stratification is also necessary.

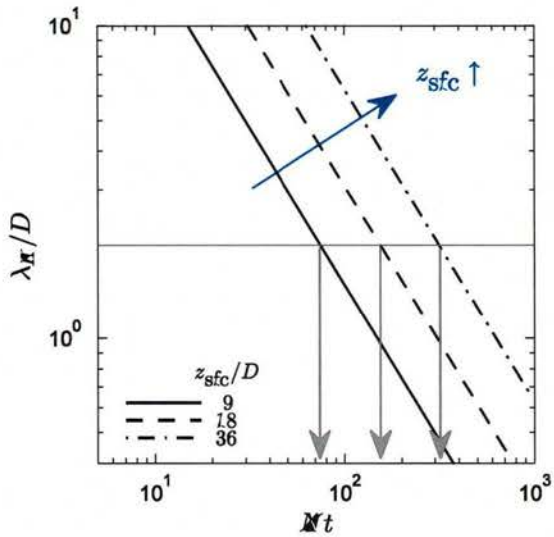

Figure 10: Time evolution of λ_H/D in Nt for various wake depths, $z_{sfc}/D \in [9, 18, 36]$, as predicted by our linear model using the calibrated virtual origin z0/D = 0.62 for waves propagating at $\theta = 45^\circ$ to the vertical. A given λ_H/D observed at the surface (marked by the horizontal grey line) may correspond to different Nt values (where the vertical grey arrows point at, for each z_{sfc}/D considered in the figure) of the submerged turbulence which may be located at various depths.

The horizontal wavelength with the highest probability of occurrence, $\hat{\lambda}_H / D$, as sampled from the peak values of the joint p.d.f.'s in Figure 7, is shown in Figure 11. For a given Re, an approximate $Fr^{1/3}$ scaling is observed, consistent with previous numerical and experimental studies. In terms of Reynolds number dependence, increasing Re by a factor of 20 at a given Fr leads to a 50% reduction in $\hat{\lambda}_H / D$. A first explanation may be offered in terms of the Ozmidov scale of the turbulence at the onset of the NEQ regime.

Additional work has been performed in terms of the potential of the surface-reflecting internal waves to generate remotely visible slicks. A 2-D Fourier-based advection solver, driven by the horizontal

velocities of the internal waves at the surface, has been run, initialized by an initial model surfactant concentration of Γ_0. The reflecting wave strain fields will then modulate this surfactant distribution and generate regions of instantaneous enhanced/reduced surfactant concentration, Γ, corresponding to values of Γ / Γ_0 greater or larger than unity. An example is shown in Figure 12, where the normalized surfactant concentration is shown along with the normalized horizontal divergence at time Nt=70 for Fr=64 and Re=10^5. In remote sensing, strain-driven concentration of Γ / Γ_0, is considered to be remotely visible slicks. We have found that high Re wakes have a pronounced tendency to generate such slicks, with this tendency increasing with Fr=64 as shown in Figure 12b.

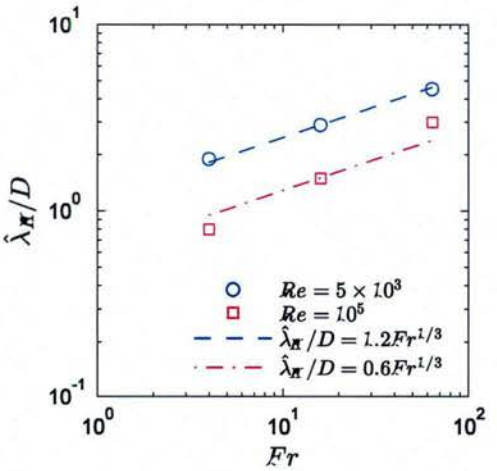

Figure 11: Fr- and Re-dependence of the most energetic wavelength $\hat{\lambda}_H / D$ observed at the sea surface.

Scaling analysis of the above advection equation shows that the normalized surfactant concentration perturbation Γ' / Γ_0 should scale with the normalized horizontal divergence, Δ_z/N, of the internal wave field. Figure 13 shows that the LES data confirms this observation. A possible leveling off of the numerical data at Re=10^5 and Fr=64 requires further investigation at parameter values that are inaccessible within current computational resources.

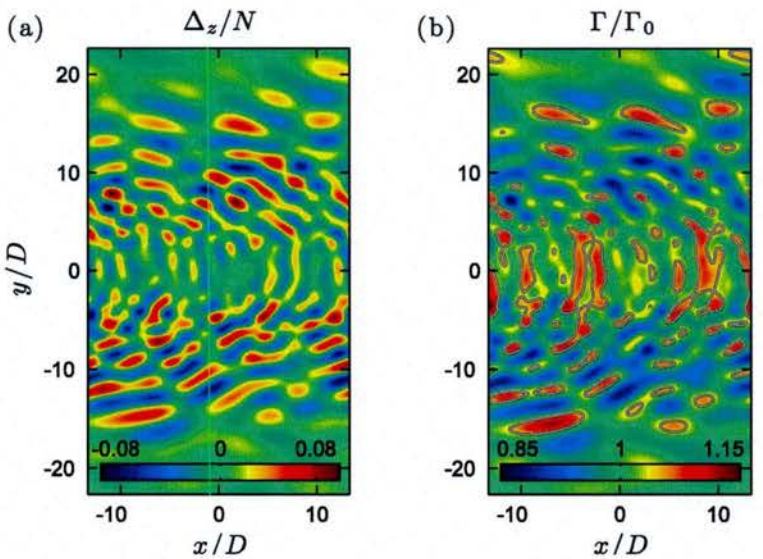

Figure 12: Surface snapshot of (a) wave-induced horizontal divergence z and (b) straindriven surfactant concentration fields at $Nt = 70$ for $Re=10^5$ and $Fr=64$. Concentration of $\Gamma / \Gamma_0 > 1.05$ may correspond to surface slicks that can be detectable via remote sensing. Isolines with $\Gamma / \Gamma_0 = 1.05$ are marked in grey, delineating possible locations of slicks.

Finally, although we have demonstrated that the wake-radiated internal waves do not undergo nonlinear effects, at least once they've left the near-field, they are still likely to be subject to such effects upon their reflection at the free surface. This hypothesis is driven by the observation of nonlinear effects (generation of harmonics and Lagrangian mean flow formation) we have observed in our idealized studies of reflecting 2-D internal wave beams. To this end, 2-D Lagrangian particle tracking has been performed on the free surface. A large number of tracer particles are inserted onto the free surface, prior to the arrival of any internal wave activity. Particles are spaced apart by $0.1D$. By virtue of the free-slip condition (w=0 at the impermeable boundary), these particles cannot be move downward and are only displace on the free surface. One may then examine the statistics of lateral particle displacement $\Delta|y^+|$. A net positive displacement suggests that any Lagrangian mean flow due to reflecting waves is sufficiently powerful to slow push particles outward away from the wake centerline.

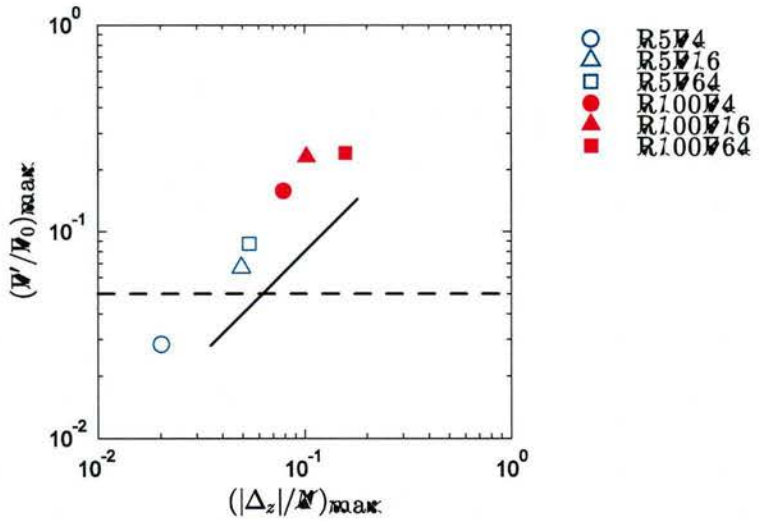

Figure 13: Peak surfactant perturbation ratio Γ' / Γ_0 versus the peak dimensionless surface strain | z|/N observed in all six simulations. Only $\Gamma' > 0$, i.e., surfactant enrichment, and z < 0, i.e., flow convergence, are considered. The characteristic enrichment ratio $\Gamma' / \Gamma_0 = 0.05$ (dash line) across observable slicks as commonly proposed in oceanographic field measurements is exceeded by all cases except for Fr=4 at the low Reynolds number. A scaling of $\Gamma' / \Gamma_0 \approx \Delta_z / N$ (solid line) can be observed.

Computational restrictions have prevented us from examining the $Re=10^5$, Fr=64 case. However, non-negligible particle drift is seen for Fr=4 and 16 at this higher Reynolds number (Figure 14). Prior to the arrival of the most energetic waves at the surface (dashed lines in Figure 14), the p.d.f. of lateral particle displacements centers around zero with some symmetric deviation. After the most intense wave impact (solid lines in Figure 14), a biased towards non-negligible particle drifts away from the wake centerline is observed. Given that nonlinear effects will increase with both Fr and Re, it is not unlikely that this particle can be as large as O(D) at operationally relevant parameter values. For an underwater

submersible, this might suggest approximately 10m displacements of surface particulates which are clearly visible through remote sensing technology.

Our findings on the surface manifestation of a submerged stratified turbulent wake may be found in the article by *Zhou and Diamessis* (*J. Fluid Mech.* 2016).

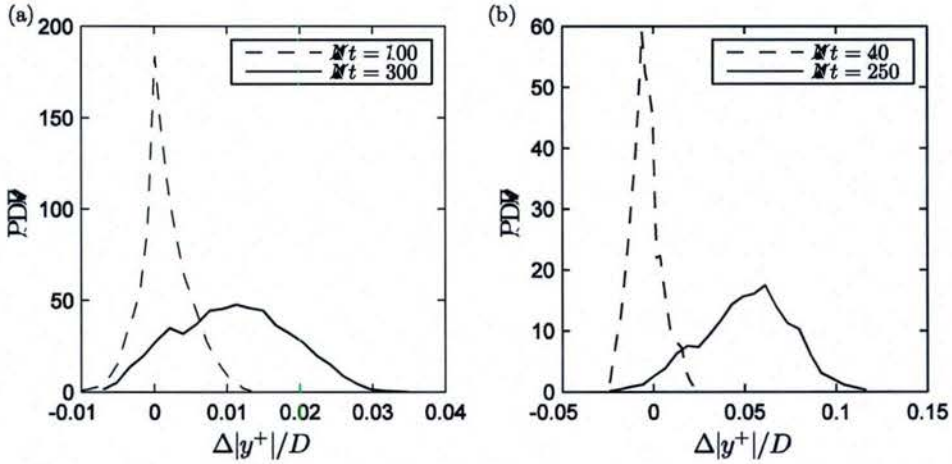

Figure 4: PDF of lateral particle displacements of away from the wake centreline at (a) Re=10^5 and Fr=4 and (b) Re=10^5 and Fr=16. Dash lines denote the PDF before the most energetic waves interact with the surface, and the solid lines the PDF after the most energetic wave impact.

(iii) Very high Reynolds number stratified wakes.

Enabled by a DoD-HPCMP Frontier grant (PI: Prof. Steve de Bruyn Kops, U. Mass., Amherst)., three simulations at Re=4×10^5 and Fr=4, 16 and 64 run up to time Nt=1,000 were completed on DoD-HPC systems using a dedicated 3,072 processor partition. These three simulations are at the highest sphere-based Reynolds number achieved so far. Moreover, they effectively provide three critically important additional points in the *(Re,Fr)* parameter space to complement existing data at the same three Fr values and Re=5×10^3 and 10^5.

Each Re=4×10^5 run required 1024×1024×1189 grid points and used 1024 cores (512 MPI processes). The choice of resolution was made to enable a broader dynamic range than what was considered in the Re=10^5 case. 10M CPU hrs were consumed in FY 2014 through meticulous simulation supervision by the PhD student funded by this grant. An approximately 20Tb large database has been generated.

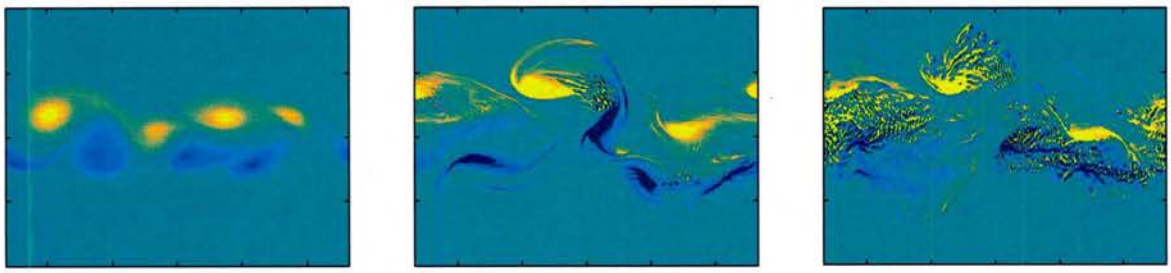

Figure 15: Contour plots of vertical vorticity ω_z at Nt=150 sampled at the *Oxy* horizontal mid-plane for simulations at $Re = 5\times10^3$, 10^5 and 4×10^5 respectively (from left to right) and Fr=4. Sphere travels from left to right. Distance between adjacent ticks on the axes is 5*D*.

Figure 15 shows example stream-span cuts for the late wake, at Nt=150. The late-time pancake vortices of low *Re* stratified wakes, typical of the laboratory, are replaced quasi-horizontal vortices carrying significant fine-structure which persists at times as late at Nt=300 at $Re=4\times10^5$. This turbulent fine-structure is intimately connected to secondary Kelvin-Helmholtz instabilities visible on stream-depth cuts, resulting from the enhanced buoyancy-induced shear at higher Reynolds numbers.

Following the pioneering work of Spedding (*J. Fluid Mech.* 1997), we have sought to identify the transition point between the NEQ and Q2D regimes, as manifested by a change in the decay power law of the mean centerline velocity U_0: at this point, the power law changes from a -1/4 to a -3/4 exponent. Although the NEQ regime appears to last consistently longer with increasing *Re*, we were unable to identify a distinct transition in exponents as postulated by Spedding.

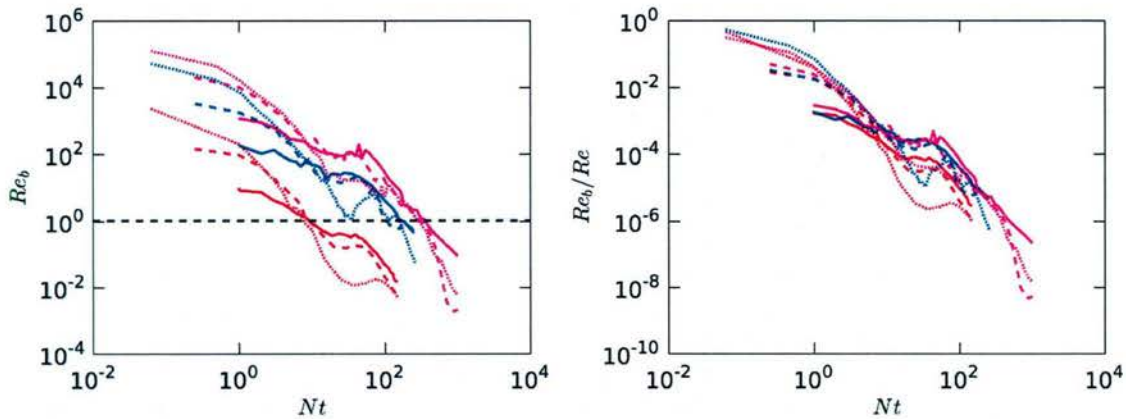

Figure 16: LEFT PANEL: Evolution of the buoyancy Reynolds number, $Re_b=Re_H Fr_H^2$, as a function of time in buoyancy units for all nine stratified wake simulations. Here Re_H and Fr_H are local Reynolds and Froude numbers based on the horizontal integral scale and characteristic horizontal velocity of the turbulence. Purple, blue and red line colors correspond to $Re=4\times10^5$, 10^5 and 4×10^5, respectively. Solid, dashed and dotted lines correspond to Fr=4, 16 and 64, respectively. RIGHT PANEL: Buoyancy Reynolds number, Re_b, rescaled with the sphere-based Reynolds number, *Re*. The key idea is that the time where Re_b crosses unity scales with *Re*, indicating that at operationally relevant *Re*, the NEQ regime, and its associated stratified turbulence, can persist over extremely long times.

More robust information on the transition point between NEQ and Q2D and, therefore, the duration of the former may be obtained by examining the buoyancy Reynolds number, R, defined in terms of characteristic horizontal velocities and the horizontal integral lengthscale of the stratified turbulence, provides further insight into the persistence of the NEQ regime (Figure 16, left panel). R is a measure of the separation between the Ozmidov (largest scale which can overturn against the restoring effect of buoyancy) and the Kolmogorov scales of the turbulence. Once it drops below a value of 1, stratified turbulence is suppressed and a transition to the Q2D has taken place. Consistently with figure 15, this crossing of the threshold occurs later with increasing Re.

Furthermore, this crossing occurs at a time that scales with Re (Figure 16, right panel). For example, if at $Re=10^5$, this transition occurs at $Nt\approx100$, at the operationally relevant value of $Re=10^8$, the transition out of the NEQ regime would take place at $Nt\approx10{,}000$. If a typical value of oceanic buoyancy frequency ranges between 0.01 and 0.1 *rad/sec* several questions emerge about the persistence of a stratified turbulent wake in the field.

Our remaining thrust area in the framework of high Re stratified wakes is the quantification of turbulent transport coefficients, i.e., horizontal and vertical eddy viscosities. These eddy viscosities are integral to rapid-turnaround self-similarity models for the prediction of downstream mean wake velocity evolution. Vorticity visualizations (see Figure 15) indicate that the horizontal spreading rates of higher Re stratified wakes might be faster than their low Re counterparts. Moreover, the presence of persistent stratified turbulence extending up to $Nt\approx300$, suggests that non-negligible vertical eddy diffusivities should be present well-after the critical time of $Nt\approx2$, the onset of the NEQ regime, after which Meunier et al. (*Phys. Fluids* 2006) proposed that the vertical Reynolds stresses go to zero. Such a proposal is clearly biased by a reliance on low Re experimental data.

The procedure of computation of the horizontal eddy viscosity is illustrated for one instant (Nt=2) for the Fr=4 and $Re=10^5$ case in Figure 17. Both the transverse gradient of the mean velocity and the horizontal Reynolds stresses are averaged along the homogeneous x-direction. For values of horizontal Reynolds stress exceeding a threshold value (40% of the max), a scatter plot of the above two quantities is constructed. A linear least squares fit to this cloud of data points has a slope which is equal to the horizontal eddy viscosity of the stratified wake at the particular time.

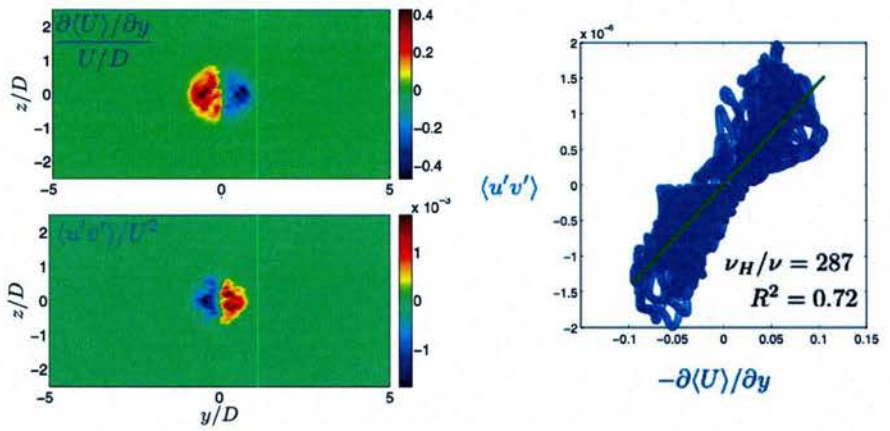

Figure 17: Left: Streamwise-averaged *yz*-transect of the lateral gradient of the mean velocity at Nt=2 for the $Re=10^5$ and Fr=4 (top). Equivalent streamwise-averaged transect of horizontal Reynolds stress field <u'v'>. Right: Scatter plot of these quantities for Reynolds stresses that exceed 40% of the maximum value. The slope of the linear least squares fit represents a measure of the eddy viscosity. R is the correlation coefficient.

Up to Nt=2, the wake behaves effectively likes its non-stratified counterpart. Hence, horizontal and vertical eddy viscosities are equal. Beyond this point, a similar procedure to the above is used to compute the vertical, buoyancy-influenced, eddy viscosity. This procedure is the object of ongoing scrutiny and discussion (see below).

The time evolution of the horizontal eddy viscosity, for all 9 cases, is shown in Figure 18. Quite curiously, the eddy viscosity departs from the typically assumed constant value at $Nt \geq 3$. Non-dimensionalizing with U_0 and L_H, mean profile quantities, does not seem to collapse the data past $Nt \approx 10$, i.e. a time when stratification has dominated the flow (Figure 18a). Moreover, the constant eddy viscosity values proposed in independently by Bevilaqua and Lykoudis (*J. Fluid Mech* 1978) and the classical textbook of Tennekes and Lumley (1972) do not seem to match our results. The former, used in the stratified wake self-similarity model of Meunier et al. (*Phys. Fluids* 2006), shows the strongest disagreement. Non-dimensionalizing with the square root of the maximum horizontal Reynolds stress and an alternative choice of characteristic lengthscale linked to the shear in the mean profile, proposed by Tennekes and Lumley, collapses the data much better (Figure 18b). The physical implications of this improved scaling are currently under investigation.

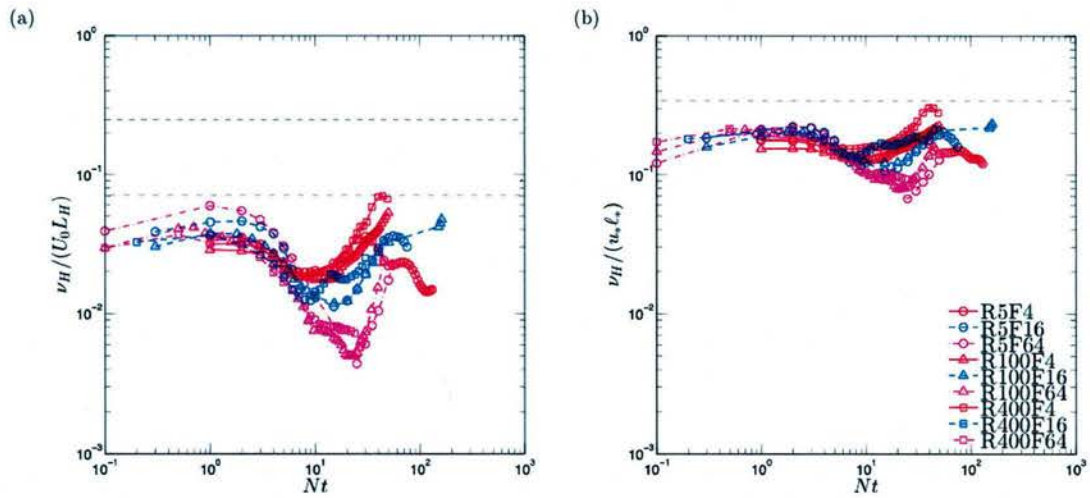

Figure 18: (a) Horizontal eddy viscosity for all 9 wake simulations, scaled with the mean centerline velocity, U_0, and the wake half-width, L_H. (b) Same quantity but scaled with u_*, the maximum horizontal Reynolds stress, and l_*, an effective Reynolds stress profile e-folding scale (see the textbook by Tennekes and Lumley).

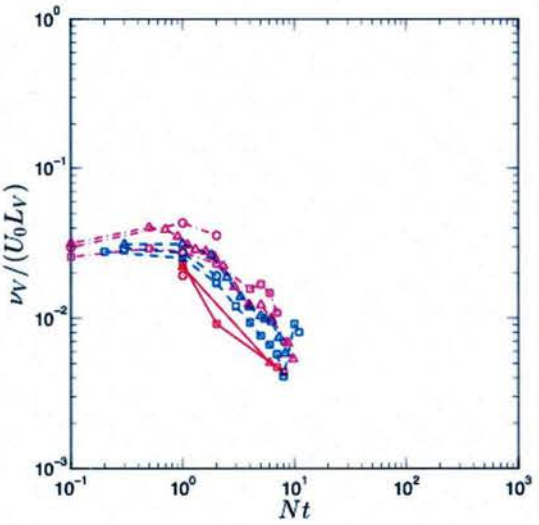

Figure 19: Vertical eddy viscosity for all nine wake simulations scaled with mean wake centerline velocity and mean profile half-height. The correlation of the least squares fit (equivalent to what is shown in Figure 14) is lost after Nt=10, presumably due to the approach used in computing the vertical eddy viscosity which does not focus on physics particular to stratified turbulence.

Results for the vertical eddy viscosity, using mean-flow-quantity-based scaling, are shown in Figure 19. The particular scaling seems to collapse the results from all 9 cases up to $Nt\approx10$. Beyond this point, any correlation in the scatter plots equivalent to the one shown in Figure 17 is lost and a no reliable slope of a linear squares fit can be computed and, therefore, no eddy viscosity estimate is possible.

It is here where it is very likely that the vertical eddy viscosity cannot be computed in a manner analogous to its horizontal counterpart. This was the focal point of the PI's discussions with Dr. Patrice Meunier during his ONR-funded summer visit to IRPHE Marseille in France. Vertical transport is dominated by z-localized processes (secondary K-H instabilities) the underlying shear of which is not identical to that of the mean flow. Hence, one must examine the rms-value of the vertical shear of the horizontal and vertical velocities to correctly account for the full effect of buoyancy-driven shear. A conditional sampling, considering local values of the Richardson number below unity, might also be necessary. Finally, it is likely that the vertical profile might not necessarily be a Gaussian and effectively the solution to the equations of high *Re* wake mean profile evolution may not be self-similar. In other words, the modified mean profile evolution equations may only be solved numerically. These issues are the focal point of our current investigations.

The most recent update on our work on high *Re* effects in stratified wakes may be found in the conference article by *Diamessis and Zhou* (2016).

(iv) Collaborative DNS/LES of high Reynolds number stratified wakes (Frontier-award support)

Beyond generating an unprecedented dataset at high *Re*, our Frontier-project-driven collaboration with Prof. de Bruyn Kops, Prof. Jim Riley (U. Washington) and Dr. Andreas Muschinski (NWRA) has advanced considerably since its initiation in Fall 2013. Apart from regular weekly discussions, the most

notable accomplishment has been Prof. de Bruyn Kops execution of a subset of DNS runs initialized by our wake data at Nt=3, 11, 21, 41 and 6 at Fr=4 and Re=10^5 and 4×10^5. Each run is conducted for a duration of Nt=2 which allows for the small-scale portion of the turbulence spectrum, unresolved by the LES, to be "filled up". Analysis of the existing DNS results by a postdoc visiting Prof. Riley has yielded significant insight on the non-trivial process of identifying the wake's non-turbulent/turbulent interface in a stratified environment, the spatial distribution of turbulence lengthscales w/r to this interfacial zone and the presence of internal wave-radiated energy that is comparable to the turbulent kinetic energy dissipation inside the wake. This work was published in *Watanabe et al.* (*J. Fluid Mech.* 2016).

Ongoing/Future Work

Current work is focused on completing the high *Re* scaling analysis of our stratified wake database as presented in section (iii) of this report. The aim is to provide a theoretical foundation for the observed scaling and a first predictive parameterization of the trajectory of a stratified turbulent wake in the turbulent Reynolds/Froude number database. A postdoctoral researcher funded by the continuation of this grant, arrived at Cornell on 4/1/2016, and has already completed systematic work on quantifying and parameterizing the internal wave energy fluxes out of a stratified turbulent wake. In parallel, the postdoc is exploring the relevant significance of these fluxes in the greater wake energy budget and is examining the potential for sound generation at high Froude numbers. As a next step, the postdoc will work on optimizing the current LES code, for optimal performance on Knight's Landing Architectures on state-of-the-art DoD HPC systems. He will also work on implementing a pilot-level strategy, currently implemented in MATLAB, for minimizing spurious divergence at spectral subdomain interfaces in the actual Fortran 90/95 code. This strategy will allow for more stable wake simulations at body-based Reynolds numbers as high as 2×10^6 which have never been attained so far.

Personnel

This ONR grant has supported one Ph.D. student for the entire course of his thesis. Dr. Qi Zhou received his PhD in May 2015. His 2-year postdoc at Cambridge U. is nearing an end. In September 2017, he will join the faculty of the Department of Civil and Environmental Engineering at the University of Calgary in Canada as an Assistant Professor. The postdoctoral researcher currently supported by the continuation of this grant is Dr. Kristopher Rowe, who was granted a PhD in Applied Mathematics by the University of Waterloo in March 2016.

Publications generated by this project

Q. Zhou (2015) "Far-Field Evolution of Turbulence-Emitted Internal Waves and Reynolds Number Effects on a Localized Stratified Turbulent Flow". *PhD thesis*, Cornell University.

Q. Zhou and P.J. Diamessis (2015) "Lagrangian flows within reflecting internal gravity waves at a free-slip surface" , *Phys. Fluids* ; 27, Article 126601.

Q. Zhou, and P.J. Diamessis (2016) "Surface manifestation of internal waves emitted by submerged localized stratified turbulence" , *Journal of Fluid Mechanics*, **798**, pg. 505-539.

T. Watanabe, J.J. Riley, S.M. de Bruyn Kops, P.J. Diamessis and Q. Zhou (2016), "Turbulent/nonturbulent interfaces in wakes in stably-stratified fluids" , *Journal of Fluid Mechanics*, **797**, R1.

P. J. Diamessis and Q. Zhou (2016) " Reynolds number effects in stratified turbulent wakes," Proc. of the 11th Intl. Sympos. on Stratified Flows, August 2016, San Diego, CA.